The Plant Cell, Vol. 3, 333–344, April 1991 © 1991 American Society of Plant Physiologists

Role of Calcium in Signal Transduction of *Commelina* Guard Cells

Simon Gilroy,[1] Mark D. Fricker,[2] Nick D. Read, and Anthony J. Trewavas[3]

Institute of Cell and Molecular Biology, University of Edinburgh, The King's Buildings, Mayfield Road, Edinburgh EH9 3JH, United Kingdom

The role of cytosolic Ca^{2+} in signal transduction in stomatal guard cells of *Commelina communis* was investigated using fluorescence ratio imaging and photometry. By changing extracellular K^+, extracellular Ca^{2+}, or treatment with Br-A23187, substantive increases in cytosolic Ca^{2+} to over 1 micromolar accompanied stomatal closure. The increase in Ca^{2+} was highest in the cytoplasm around the vacuole and the nucleus. Similar increases were observed when the cells were pretreated with ethyleneglycol-bis-(*o*-aminoethyl)tetraacetic acid or the channel blocker La^{3+}, together with the closing stimuli. This suggests that a second messenger system operates between the plasma membrane and Ca^{2+}-sequestering organelle(s). The endogenous growth regulator abscisic acid elevated cytosolic Ca^{2+} levels in a minority of cells investigated, even though stomatal closure always occurred. Ca^{2+}-dependent and Ca^{2+}-independent transduction pathways linking abscisic acid perception to stomatal closure are thus indicated.

INTRODUCTION

Carbon dioxide uptake for photosynthesis and water loss via transpiration occur primarily through stomatal pores in the leaf epidermis. Regulation of this gaseous exchange is achieved through changes in stomatal aperture in response to the complex interaction of a wide variety of stimuli. In particular, light and low levels of CO_2 stimulate stomatal opening, whereas high levels of CO_2, darkness, or ABA cause closure (Raschke, 1975; Zeiger, 1983). ABA levels increase under water stress and, therefore, may link stomatal responses to plant water status (Davies et al., 1981).

Stomatal movements result from changes in the osmotic potential and, hence, turgor of the two guard cells surrounding the pore. These changes occur through modulation of both ion fluxes across the plasma membrane and tonoplast and the rate of synthesis or degradation of osmotically active solutes in the cytoplasm (MacRobbie, 1988; Hedrich and Schroeder, 1989; Schroeder and Hedrich, 1989). The precise mechanism(s) by which these processes are controlled and integrated is unclear.

The involvement of a Ca^{2+}-based signal transduction pathway in guard cell responses has been the subject of considerable interest (reviewed by Mansfield et al., 1990). Elevated levels of extracellular calcium ($[Ca^{2+}]_e$) directly stimulate stomatal closure or reduce stomatal opening in response to light (De Silva et al., 1985b; Schwartz, 1985), K^+ (Inoue and Katoh, 1987), or low CO_2 (Schwartz et al., 1988). Conversely, closure in response to darkness (Schwartz, 1985), elevated CO_2 (Schwartz et al., 1988), and ABA (De Silva et al., 1985b) is inhibited by incubation in EGTA. Stomatal closure is also stimulated by the Ca^{2+}-ionophore A23187 (De Silva et al., 1985a) and inhibited by Ca^{2+} channel blockers (De Silva et al., 1985a; Inoue and Katoh, 1987). McAinsh et al. (1990) reported that cytosolic Ca^{2+} levels ($[Ca^{2+}]_i$) variably increased with ABA in eight out of 10 guard cells examined.

We have recently shown that cytoplasmic release of Ca^{2+} or inositol trisphosphate (IP_3) from their caged forms can initiate stomatal closure. Both of these treatments led to an increase in $[Ca^{2+}]_i$ but only triggered stomata to close when $[Ca^{2+}]_i$ rose to above a threshold of approximately 500 nM to 600 nM (Gilroy et al., 1990). ABA-induced increases would have to be above this level to contribute significantly to the closure mechanism. Furthermore, direct measurement of $^{45}Ca^{2+}$ fluxes into guard cells showed ABA to have variable effects on Ca^{2+} influx ranging from stimulation to inhibition (MacRobbie, 1989). ABA also has been reported to cause shrinkage of guard cell protoplasts (analogous to stomatal closure) in the absence of $[Ca^{2+}]_e$ (Smith and Willmer, 1988). These latter results do not support a requirement for trans-plasma membrane Ca^{2+} influx in transduction of the ABA response but do not preclude the modulation of $[Ca^{2+}]_i$ through mobilization of internal Ca^{2+} stores. Although closure can be initiated by

[1] Current address: Department of Plant Biology, University of California, Berkeley, CA 94720.

[2] Current address: Department of Plant Sciences, University of Oxford, South Parks Road, Oxford OX1 3RA, United Kingdom.

[3] To whom correspondence should be addressed.

A23187 or increased $[Ca^{2+}]_e$ or be inhibited by EGTA, there are no measurements in plant cells that show that these treatments do initiate their assumed effects upon $[Ca^{2+}]_i$. Ionomycin, a more specific Ca^{2+} ionophore than A23187 (Thomas, 1982), does not initiate closure unless very high concentrations (100 μM) are used (M.D. Fricker and S. Gilroy, unpublished results) and was not observed to increase guard cell $[Ca^{2+}]_i$ in vivo (McAinsh et al., 1990). $[Ca^{2+}]_e$ is known to have nonspecific effects on membrane permeability (Zhao et al., 1987), and both $[Ca^{2+}]_e$ and EGTA can have direct effects on cell wall structure and stiffening. Such uncertainties highlight the need to measure directly the dynamics and the spatial location of $[Ca^{2+}]_i$ inside cells when perturbed by ionophores or other closing treatments.

Fluorescence ratio analysis is an entirely new technology that enables the direct visualization and precise measurement of changes and spatial distributions of $[Ca^{2+}]_i$ inside single living cells (Tsien and Poenie, 1986; Cobbold and Rink, 1987; Bush and Jones, 1990). The technique can, therefore, detect mobilization of $[Ca^{2+}]_i$ from organelles and help resolve the issue of the putative origin of $[Ca^{2+}]_i$ during closure. We have used it here for this purpose. Furthermore, if organelle $[Ca^{2+}]_i$ mobilization can be induced by stimuli acting at the plasma membrane, this might help to clarify whether second messengers such as IP_3 act in guard cell signal transduction. Our demonstration that release of IP_3 from its caged form in guard cells mobilizes $[Ca^{2+}]_i$ is suggestive of this possibility but needs much more substantiation (Gilroy et al., 1990; Irvine, 1990). Fluorescence ratio imaging or photometry can, thus, enable quantitative measurements of $[Ca^{2+}]_i$ in guard cells after treatment with ionophores, $[Ca^{2+}]_e$, EGTA, or other treatments.

Besides ABA, light and CO_2 are considered the two primary regulators of stomatal aperture. Because fluorescence ratio imaging necessitates exposing cells to ultraviolet light, observations on putative ultraviolet/blue light regulation of internal calcium stores are precluded. Furthermore, the optical specifications of fluorescence ratio imaging or photometry require perfusion of the tissue in liquid media in an open chamber. Thus, accurate control of aperture by CO_2 levels is difficult. We have, therefore, manipulated stomatal aperture by extracellular K^+ and Ca^{2+}, both of which are potential physiologically relevant stimuli. Apoplastic levels of Ca^{2+} in the epidermis are regulated in vivo in *Commelina communis* and have been proposed as a physiological controlling stimulus (Atkinson et al., 1989). Although the actual extracellular concentration of K^+ in the stomatal apoplast is still controversial (Blatt, 1985; Bowling, 1987), there are significant (30-fold) variations during closure that could exert significant feedback on stomatal behavior. We have used these stimuli and ABA to try to detect organelle $[Ca^{2+}]_i$ mobilization and, thus, to clarify the mechanism of ABA action. Our results are surprising. Although we could obtain good evidence for internal $[Ca^{2+}]_i$ mobilization, we could not detect consistent effects of ABA on $[Ca^{2+}]_i$. The findings indicated that both Ca^{2+}-dependent and Ca^{2+}-independent pathways link ABA perception to stomatal closure.

RESULTS

Guard Cell Function Is Unaffected by Loading with Indo-1

For the unequivocal interpretation of ratio analysis data, it is essential to establish that (1) the ratio dye is localized in the cytosol, (2) the cell remains unperturbed by the dye-loading and ratio analysis procedures, and (3) the measurement procedure has not altered the cellular response. We tested three methods to load the guard cell cytosol with the Ca^{2+}-sensitive fluorescent dyes Indo-1 and Fura-2 (Grynkiewicz et al., 1985): ionotophoretic microinjection, the dyes as acetoxymethyl esters, and use of the low pH method of Bush and Jones (1988). Microinjection of Indo-1 was found to be the most successful and reliable method. Both ester and acid loading failed to show measurable uptake of Indo-1 fluorescence into the cytoplasm even at 100 mM dye concentration. We also observed an apparent irreversible binding of the dye to the guard cell wall. This bound dye was not accessible to changes in medium Ca^{2+}, Ca^{2+} ionophores, or quenching by Mn^{2+}.

Microinjection caused minimal disruption of the cell wall at the site of penetration, and dye loading did not appear to alter stomatal responses as judged by the following criteria: (1) injected guard cells remained turgid and similar in shape to the noninjected guard cell of the stoma, as shown in Figures 1 and 2; (2) there was no evidence of papilla formation at the site of microinjection (Figure 1); (3) there was no observable difference in organelle shape or distribution between injected guard cells and noninjected controls (Figure 1); (4) injected cells remained viable throughout all of the experimental treatments as judged by neutral red staining (data not shown); (5) saltatory movements of organelles continued after microinjection; and (6) as Figure 3 shows, the kinetics of responses to Ca^{2+}, EGTA, and ABA revealed no significant difference between dye-loaded cells and nonloaded controls.

Figure 2A shows the characteristic fluorescence from a guard cell microinjected with Indo-1 into the cytoplasm. The dye diffused from the site of microinjection and became evenly distributed throughout the cytosol within 10 min. The nucleus exhibited much stronger fluorescence than the cytosol. No punctate fluorescence, as might be expected if chloroplasts or mitochondria accumulated the dye, was observed within 1 hr. All further experiments were conducted within this time period. Successful dye loading into the cytoplasm produced no discernible signal from the vacuole (Figure 2A).

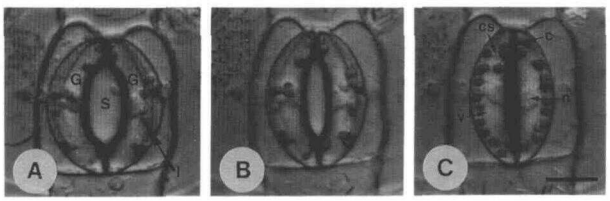

Figure 1. Differential Interference Contrast Light Micrographs of a Guard Cell Pair during Stomatal Closure.

(A), **(B)**, and **(C)** The same cell imaged at 0 min, 30 min, and 60 min, respectively, after the addition of 1 μM ABA. The right guard cell in each section was ionotophoretically microinjected with Indo-1; the left guard cell represents an uninjected control. The cytoplasm forms a thin layer around the periphery of the cell with fine strands crossing the vacuole. G = guard cell; S = stomatal pore; I = point of microinjection; n = nucleus; c = chloroplast; v = vacuole; cs = cytoplasmic strand. Scale bar = 10 μm.

For comparison, Figure 2B shows a cell, which would normally be rejected for further analysis, with dye injected into the vacuole. Vacuolar Indo-1 was Ca^{2+} saturated and, thus, over 1 μM in concentration (Elliott and Petkoff, 1990). The overall fluorescence intensity was greater than for the cytoplasmically injected cell. The fluorescence distribution was altered, being excluded from the nucleus and chloroplasts that were negatively stained. The cell also showed a marked loss of turgor, which was not evident in successful cytosolic injections.

Spatially Localized Increases in Cytosolic Ca^{2+} Concentration Precede Stomatal Closure

Stomatal apertures can be closed reversibly by increasing $[Ca^{2+}]_e$ or by treatment with the Ca^{2+} ionophore A23187 (De Silva et al., 1985a, 1985b; Schwartz, 1985; Inoue and Katoh, 1987; Schwartz et al., 1988). These observations suggest that changes in $[Ca^{2+}]_i$ may be involved in aperture control. However, in neither case has the critical experiment of directly demonstrating the modulation of $[Ca^{2+}]_i$ been performed.

Figure 4B shows photometric measurements of $[Ca^{2+}]_i$ in guard cells when $[Ca^{2+}]_e$ was increased from 20 μM to 1 mM. This change induced a steady rise in the average $[Ca^{2+}]_i$ from resting levels (180 $\pm$ 52 nM) to a maximum of 600 $\pm$ 78 nM (n = 5) over a 5-min to 10-min period. Subsequently, stomatal aperture decreased (Figure 3A). An equivalent experiment in which Br-A23187, a nonfluorescent Ca^{2+} ionophore, was added to the perfusing medium in the presence of 20 μM $[Ca^{2+}]_e$ is shown in Figure 4A. Cytosolic Ca^{2+} was elevated to micromolar levels in 1 sec to 2 sec, implying that the increase in $[Ca^{2+}]_i$ observed in Figure 4B could have resulted simply from accelerated Ca^{2+} influx at the plasma membrane. Again, stomatal closure was seen to begin some 15 min after the increase in $[Ca^{2+}]_i$, and the treated cells remained viable, as judged by neutral red staining (data not shown), throughout the experimental observation period.

Photometric measurements cannot distinguish easily between accelerated Ca^{2+} influx at the plasma membrane or mobilization of Ca^{2+} from organelles, either of which could account for the results. However, imaging the distribution might distinguish more clearly between the two possibilities. Figure 5A shows an example of a cell imaged at intervals up to 30 min after changing the $[Ca^{2+}]_e$. The time points for the images presented were chosen as representative of the effect on $[Ca^{2+}]_i$ from the photometric measurements (Figure 4B). Within 2.5 min, elevation of Ca^{2+} in discrete cytoplasmic areas ("hot spots") could be seen, reaching a maximum at 10 min. Confocal microscopy has shown that the nucleus is surrounded by an extensive endomembrane system and the vacuole forms a single compartment running throughout the *C. communis* guard cell (Fricker et al., 1991). The thin layer of cytoplasm directly above the vacuole gave an extremely weak fluorescence signal, below the threshold set for accurate data collection. Therefore, measurement of $[Ca^{2+}]_i$ was not possible in these regions. These areas of greatest vacuolar depth are indicated by the dark insets within the pseudocolored cells in Figures 5A to 5E. The highest localized increases in $[Ca^{2+}]_i$ (>1 μM) were evident in the region of the cytosol around the concentration of the endomembrane system and the vacuole membrane adjacent to the

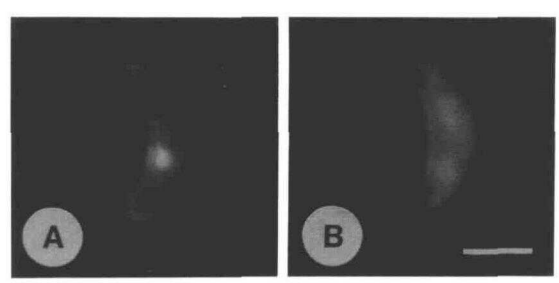

Figure 2. Fluorescence Light Micrographs of *C. communis* Guard Cells Loaded with Indo-1.

(A) Ionotophoretic microinjection of dye into the cytosol of the right guard cell. An artifactual reflection of the intense nuclear fluorescence can be seen in the thick cell wall bordering the stomatal pore. This is also evident in the ratio images (Figure 5) but does not contribute to the cytosolic Ca^{2+} signal. Note also the autofluorescence of the t-shaped junctions of the two guard cells and of the thick cell wall bordering the stoma in the noninjected guard cell.

(B) Ionotophoretic microinjection of Indo-1 into the vacuole of the right guard cell. This shows exclusion of dye from the nucleus and chloroplasts. Fluorescence was excited at 350 nm (10-nm half-bandwidth interference filter) and emission >430 nm was recorded. Scale bar = 10 μM.

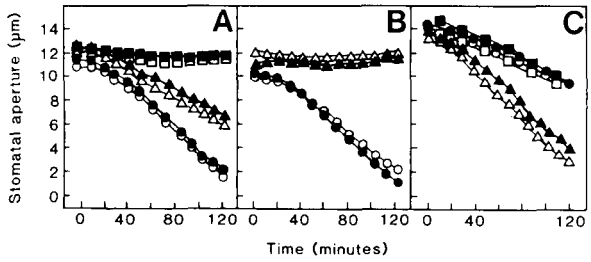

Figure 3. Kinetics of Stomatal Closure on Treatment with Increased $[Ca^{2+}]_e$, Br-A23187, EGTA, Decreased $[K^+]_e$, and ABA.

Guard cells around an open stomata were ionotophoretically microinjected with Indo-1 (white symbols) and compared with uninjected guard cells (black symbols).
(A) Untreated (□), increase in $[Ca^{2+}]_e$ from 20 μM to 1 mM Ca^{2+} with (△) or without (○) a 15-min pretreatment with 1 mM La^{3+}.
(B) Treatment with 1 mM EGTA (△) or 10 μM Br-A23187 (○).
(C) Treatment with 1 μM ABA (△) or reduction in $[K^+]_e$ from 50 mM to 25 mM with (□) or without (○) a 15-min pretreatment with 1 mM EGTA.
All treatments were instituted at zero time. At each time point, maximum apertures (pore widths) were measured from bright-field images of the stomatal complex using the video camera and image analyzer. Apertures are the average result of three to six measurements. Standard errors in every case were less than 2 μm and, for clarity, are not shown.

nucleus (Figures 5A to 5C). This elevated $[Ca^{2+}]_i$ may originate from organelles or result from influx of Ca^{2+} through clustered plasma membrane Ca^{2+} channels. Stomatal apertures in this experiment are shown in black and white micrographs of bright-field images for each time point, and elevation of $[Ca^{2+}]_i$ can again be seen to precede stomatal closure.

To distinguish more clearly the origin of these hot spots of $[Ca^{2+}]_i$, we have carried out closure imaging experiments in the presence of the Ca^{2+} channel blocker La^{3+} and in the presence of EGTA to remove apoplastic Ca^{2+}. MacRobbie (1989) has reported a ninefold inhibition of Ca^{2+} influx into guard cells by 1 mM La^{3+}. Figure 4C shows that an increase in $[Ca^{2+}]_i$ is induced by elevation of $[Ca^{2+}]_e$ from 20 μM to 1 mM in the presence of 1 mM La^{3+}, although the increase is slower (to 300 nM in 10 min). Stomatal closure occurs but is also delayed compared with treatments with Ca^{2+} alone (Figure 3A). Figure 5B presents ratio images at selected times after the elevation of $[Ca^{2+}]_e$ in the presence of La^{3+}. Spatial inhomogeneities are definitely visible in the cytosol in the vicinity of the nucleus, but their appearance is delayed by the treatment with La^{3+}, as was the overall $[Ca^{2+}]_i$ increase shown in Figure 4C. If the hot spots in Figures 5A and 5B are the result of Ca^{2+} influx through the plasma membrane that induces organelle Ca^{2+} release (Berridge and Irvine, 1989), then the data in Figure 5B suggest that only very small increases in the rate of Ca^{2+} influx are required for this process to occur. Furthermore, the Ca^{2+} influx rates from 20 μM $[Ca^{2+}]_e$ are insufficient to induce either hot spots or stomatal closure. Alternatively, the observations may be interpreted to suggest that messenger molecules other than Ca^{2+} operate between the plasma membrane and organelles.

The question can be resolved better by perfusion of guard cells with EGTA to remove freely available apoplastic

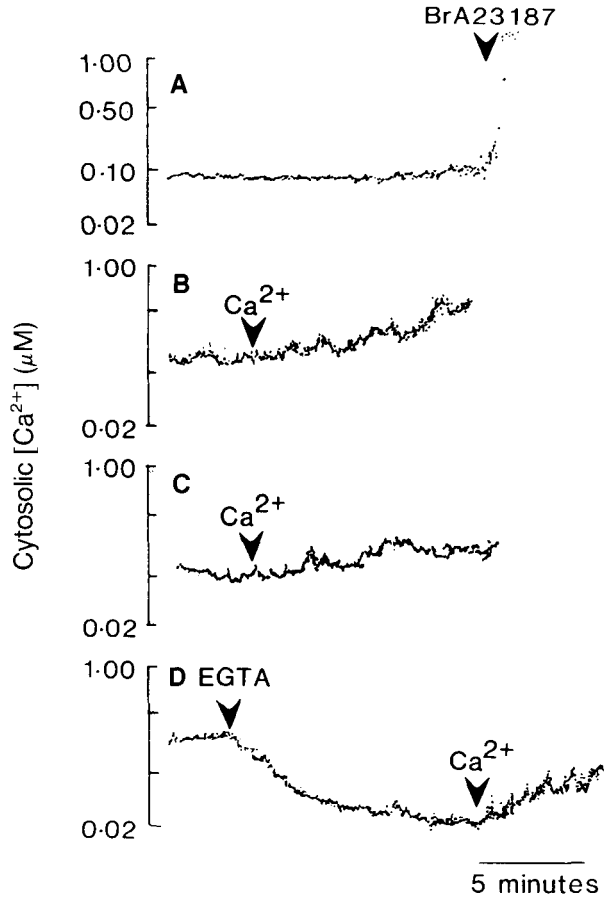

Figure 4. Photometric Measurements of $[Ca^{2+}]_i$ after Treatment of Guard Cells with Br-A23187, Increasing $[Ca^{2+}]_i$ in the Presence or Absence of La^{3+} or EGTA.

(A) 10 μM Br-A23187.
(B) $[Ca^{2+}]_e$ increased from 20 μM to 1 mM.
(C) $[Ca^{2+}]_e$ increased from 20 μM to 1 mM after a 15-min preincubation with 1 mM $LaCl_3$, which was maintained throughout the experiment.
(D) 1 mM EGTA, which was replaced by medium containing 20 μM Ca^{2+} at the right-hand arrow.
Treatments were applied at the times indicated by the arrows. The scale on each trace is identical but for clarity only the extremes are shown in **(B)** to **(D)**. The results are representative of four or more separate experiments.

Ca^{2+}. Experiments were carried out at pH 6.1. At this pH, the affinity of EGTA for Ca^{2+} is weaker than at neutral pH levels. To counteract this, epidermal strips were continuously perfused with buffer containing EGTA, thus providing an effective buffering and sequestering capacity for apoplastic Ca^{2+}. Figure 4D shows the effect on $[Ca^{2+}]_i$ of removing the apoplastic Ca^{2+} by perfusing the guard cell with 1 mM EGTA . The resting level of 220 nM was reduced over 10 min to 50 nM, indicating that EGTA acts as a physiological chelating agent. This effect was reversed by replacing the EGTA with 20 μM Ca^{2+}, as indicated by the right-hand arrow. In addition, ratio images of the EGTA-treated cells during this period indicated that the reduction in $[Ca^{2+}]_i$ was uniform over the whole cell (data not shown). During the EGTA treatment, the stomatal aperture was observed to remain constant or to increase slightly (Figure 3A). The rapid decline in $[Ca^{2+}]_i$ induced by EGTA suggests that the cytosolic pool of Ca^{2+} is in a state of continual flux and exchange with $[Ca^{2+}]_e$.

Experiments to observe the effect of EGTA on mobilization of Ca^{2+} from organelles clearly cannot also involve perturbations of $[Ca^{2+}]_e$. Therefore, we employed an alternative method, lowering the extracellular K^+ concentration ($[K^+]_e$), which is known to initiate stomatal closure when $[Ca^{2+}]_e$ is held constant. Figure 6A indicates that when $[K^+]_e$ was lowered from 50 mM to 25 mM in the presence of constant (20 μM) $[Ca^{2+}]_e$, cytosolic Ca^{2+} levels increased rapidly from resting levels (160 nM) to 700 nM over 15 min and the stomatal aperture closed subsequently (Figure 3C). Representative images of the time course of the effects of lowering$[K^+]_e$ are shown in Figure 5C. Again, spatially localized hot spots of high $[Ca^{2+}]_i$ were apparent in the cytosol around the nucleus. These hot spots can be visualized clearly in the 10-min image and were visible within 2 min of changing the $[K^+]_e$, although these data are not shown in Figure 5C.

Figure 6B records the variation in $[Ca^{2+}]_i$ when the guard cells were perfused with 1 mM EGTA for 15 min before a reduction in $[K^+]_e$ to 25 mM at zero time. The kinetics of $[Ca^{2+}]_i$ increase were similar to those in the absence of EGTA (Figure 6A), suggesting that reductions in $[K^+]_e$ led to organelle Ca^{2+} mobilization. This was confirmed by the imaging data shown in Figure 5D. The highest $[Ca^{2+}]_i$ is again within the vicinity of the vacuolar membrane and endomembrane system, but the effects are not as localized as those shown in Figure 5C. Because our data in Figure 4D indicate that the cytosolic Ca^{2+} pool is mobilized rapidly out of the cell when treated with EGTA, a reduction in the amplitude of any localized changes in $[Ca^{2+}]_i$ may be due to a rapid loss of the elevated $[Ca^{2+}]_i$ to the EGTA in the medium. Stomata closed upon reducing $[K^+]_e$ in the presence or absence of EGTA with similar kinetics (Figure 3C). This suggests that if stomatal aperture is regulated by $[Ca^{2+}]_i$, the increases observed in Figure 5D are sufficient to initiate the physiological processes of closure. Because the concentration of apoplastic Ca^{2+} will be very low in the EGTA experiments, these data suggest strongly that the mobilization of organelle Ca^{2+} requires a signal issuing from the plasma membrane that is not Ca^{2+} itself. We have no clear indication of the nature of this signal, but we have shown that release of IP_3 from its caged form induces mobilization of $[Ca^{2+}]_i$ (Gilroy et al., 1990), mimicking some of the properties of this signal. Further experiments on IP_3 in guard cells are warranted.

We also conducted experiments in which $[K^+]_e$ was lowered in the presence of La^{3+}. Similar localized increases in $[Ca^{2+}]_i$ occurred (data not shown) within several minutes after changing $[K^+]_e$, which agrees with the hypothesis that the signal induced by lowering the $[K^+]_e$ is transduced through organelle Ca^{2+} mobilization.

Is ABA-Induced Stomatal Closure Preceded by Increases or Relocalization of $[Ca^{2+}]_i$?

ABA, an endogenous growth regulator, is known to initiate stomatal closure in a variety of plants. The evidence from inhibitor studies (e.g., De Silva et al., 1985a, 1985b) and a recent photometric study shows that ABA initiated changes in $[Ca^{2+}]_i$ in eight out of 10 guard cells (McAinsh et al., 1990). The response of guard cells to increases in $[Ca^{2+}]_e$, demonstrated in this study, would clearly support this hypothesis if ABA acts through Ca^{2+}. Therefore, we sought to use ABA as a perturbing stimulus to investigate further the process whereby Ca^{2+} is mobilized from guard cell organelles.

We have made imaging and photometry measurements on 54 cells treated with a range of ABA concentrations from 100 nM to 10 μM. The photometric data are shown in Figure 7. Stomatal closure occurred in all cases (Figure 3C). However, we observed large increases in $[Ca^{2+}]_i$ (up to 1 μM) accompanied by extensive oscillations (average duration, 60 sec; periodicity, 180 sec) in only four cells. A variable set of transient rises in $[Ca^{2+}]_i$ was observed in another 10 cells. (A typical trace is shown in Figure 7.) No change in $[Ca^{2+}]_i$ was observed in the other 24 cells. Attempts to capture these ABA-induced changes in $[Ca^{2+}]_i$ by imaging have not been successful ($n = 16$ cells). Images of the cell showing the greatest variation are presented in Figure 5E. These data indicate that the modulation of stomatal aperture by ABA and $[Ca^{2+}]_i$ may not be strongly coupled.

DISCUSSION

We have visualized Ca^{2+} concentrations in single guard cells of *C. communis* using dual emission fluorescence ratio analysis after microinjection of Indo-1. The guard cells were living and functioned normally during the period of analysis. The resting $[Ca^{2+}]_i$ was maintained at a stable

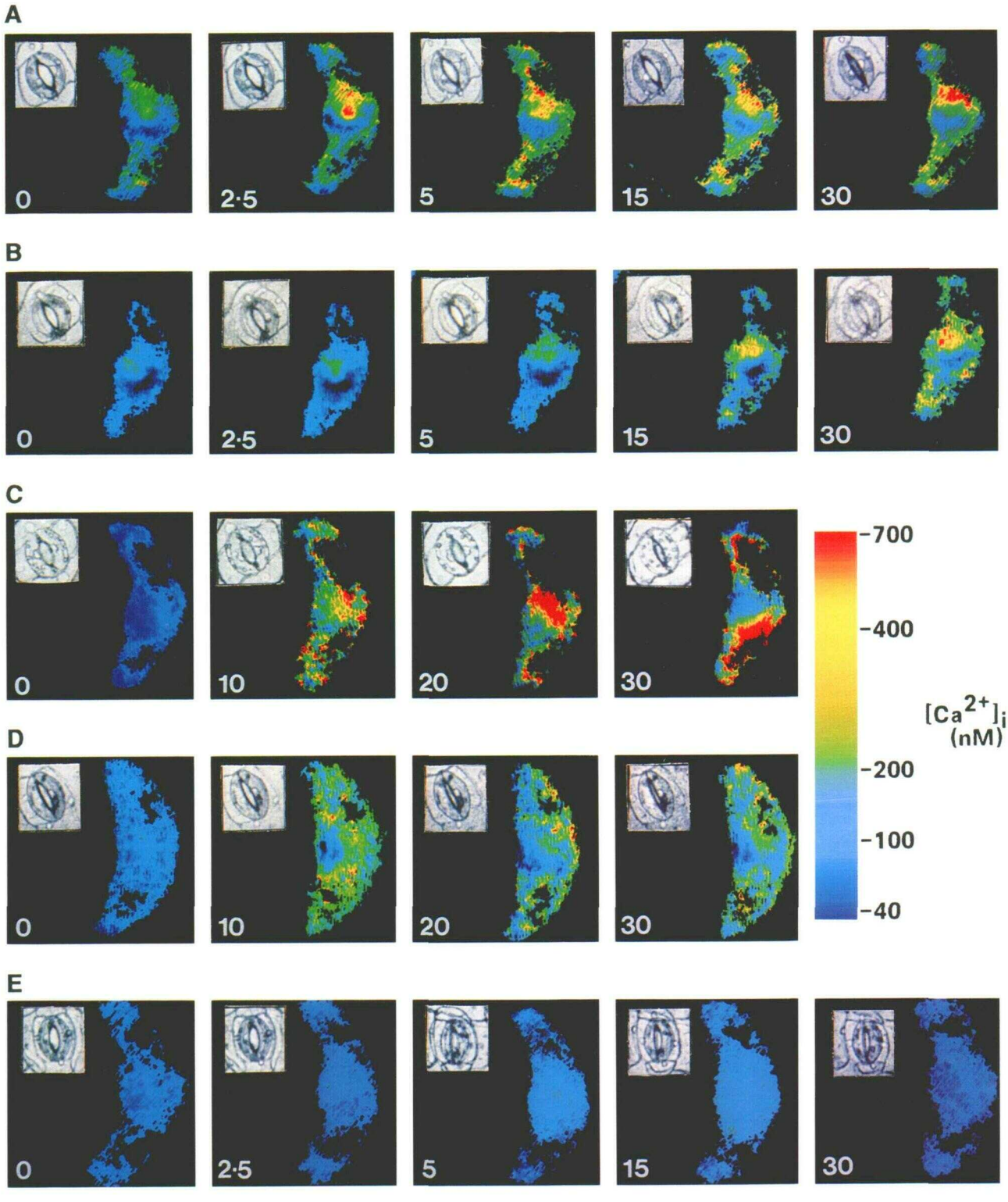

Figure 5. Fluorescence Ratio Images of the Distribution of Cytosolic Ca^{2+} in Guard Cells Loaded with Indo-1.

(A) $[Ca^{2+}]_e$ increased from 20 μM to 1 mM.
(B) $[Ca^{2+}]_e$ increased from 20 μM to 1 mM after a 15-min preincubation with 1 mM $LaCl_3$, which was maintained throughout the experiment.
(C) $[K^+]_e$ reduced from 50 mM to 25 mM.
(D) $[K^+]_e$ reduced from 50 mM to 25 mM after a 15-min preincubation with 1 mM EGTA, which was maintained throughout the experiment.
(E) Addition of 1 μM ABA.

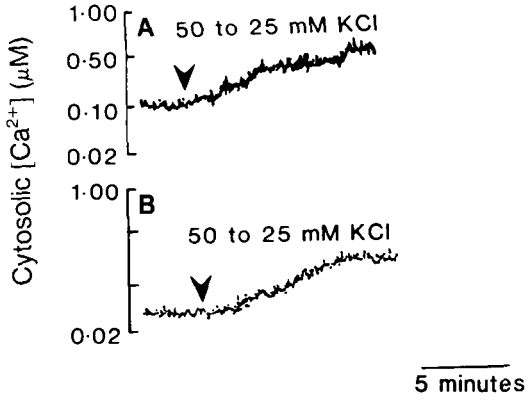

Figure 6. Fluorescence Ratio Photometric Measurements of Changes in $[Ca^{2+}]_i$ in Guard Cells Microinjected with Indo-1 after the Reduction of $[K^+]_e$ from 50 mM to 25 mM.

(A) Without EGTA treatment.
(B) With a 15-min pretreatment of 1 mM EGTA, which was maintained throughout the experiment.
Traces are representative of five or more experiments.

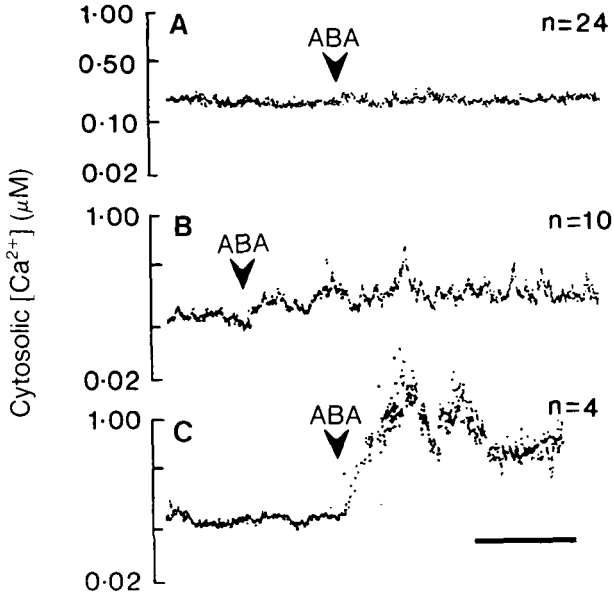

Figure 7. Changes in $[Ca^{2+}]_e$ on Treatment of Indo-1-Loaded Guard Cells with 1 μM ABA.

Guard cells around open stomata were treated with 1 μM ABA at the times indicated by the arrows. Traces representative of each class of response are shown along with the number of experiments in which they were observed. Bar = 5 min.

level of 173 ± 43 nM measured by photometry (n = 50) or 117 ± 38 nM by imaging (n = 25). The apparent disagreement between these two values may arise from the differences in the sensitivities of the measurement systems. MacRobbie (1989) calculated that the total cytoplasmic pool of Ca^{2+} in guard cells of *C. communis* was 5.7 mM from analysis of $^{45}Ca^{2+}$ flux data. Therefore, considerable sequestration and buffering of $[Ca^{2+}]_i$ must occur to maintain the submicromolar levels reported here. We can also conclude that the Indo-1 concentration in the cytoplasm in this study (<10 μM, calculated as detailed in the experimental procedures) would contribute a negligible increase in the Ca^{2+} buffering capacity of the cytoplasm, particularly because Speksnijder et al. (1989) have shown that injection of >100 μM concentrations of Indo-1-related Ca^{2+} buffers is required to interfere with zygote development in *Pelvetia*.

Is There a Second Message in the Guard Cell That Acts between the Plasma Membrane and Organelles?

In five different experimental treatments (raising $[Ca^{2+}]_e$, raising $[Ca^{2+}]_e$ plus La^{3+}, Ca^{2+} ionophore treatment, lowering $[K^+]_e$, and lowering $[K^+]_e$ plus EGTA), a clear correlative relationship emerged between elevation of $[Ca^{2+}]_i$ and closure. With our recent demonstration that an increase of $[Ca^{2+}]_i$ by release of Ca^{2+} or IP_3 from caged forms initiates closure (Gilroy et al., 1990), this relationship is now well established. Furthermore, we also observed that a transient increase in $[Ca^{2+}]_i$ greater than 0.5 μM for about 10 min is sufficient to initiate and subsequently to maintain closing events. In these cases, Ca^{2+} acts as a trigger for the events associated with closure. We also demonstrated that changes in $[Ca^{2+}]_e$ and $[K^+]_e$ increase $[Ca^{2+}]_i$ in the presence of the channel blocker La^{3+} or EGTA. On this basis, it seems unlikely that Ca^{2+} entering the plasma membrane is responsible for inducing $[Ca^{2+}]_i$ increases, as would happen in Ca^{2+}-induced Ca^{2+} increase (Berridge and Irvine, 1989), and some other message may be transmitting the information. At present, IP_3 is a good candidate for such a second message, and current data (Alexandre et al., 1990; Blatt et al., 1990; Gilroy et al.,

Figure 5. (continued).

Guard cells (microinjected with Indo-1) were treated at zero time. Ratio images were taken at the times (in minutes) indicated on each picture. Bright-field images of the stomata under study are shown (insets). The $[Ca^{2+}]_i$ has been coded according to the color scale given. Each set of images is representative of at least three experiments. The dark inserts within the pseudocolored guard cells represent the thinnest regions of cytoplasm over the vacuole where the signal strength was insufficient to provide precise ratio values. Ratio image magnifications ×325.5.

1990; Irvine, 1990) support this notion. A search for phospholipase C and IP_3 in the guard cell should be undertaken to examine this possibility more closely. Furthermore, the possible organelle origin of the $[Ca^{2+}]_i$ that increases in the nuclear region needs to be resolved more precisely from a spatial perspective, perhaps by fluorescence ratio confocal microscopy of Indo-1.

Closure is recognized as the result of turgor loss by the stomatal guard cells due to efflux of principally K^+ and Cl^- (MacRobbie, 1989). These fluxes are determined by the relative activities of ion channels and the H^+/ATPase, both of which can be modulated by Ca^{2+}. Increases in $[Ca^{2+}]_i$ to above 0.2 μM can activate ion efflux channels at both the tonoplast and plasma membrane in *Vicia* guard cells (Hedrich and Neher, 1987; Hedrich et al., 1988; Keller et al., 1989; Schroeder and Hagiwara, 1989). Ca^{2+} also has been shown to inhibit a possible plasma membrane proton pumping ATPase, although the K_i (about 200 μM) is probably too high to be of physiological significance (Nejidat et al., 1986).

A relationship between the rate and magnitude of the $[Ca^{2+}]_i$ increase and the steady rate of stomatal closure might be expected if $[Ca^{2+}]_i$ were solely responsible for controlling both the activity of the ion channels and the H^+/ATPase that regulate closure. However, the activities of the metabolic events that regulate closure are known to be constrained by other factors including external $[K^+]$, $[H^+]$, membrane potential, and energy supply (Weyers et al., 1982). Therefore, a simple relationship between the kinetics in $[Ca^{2+}]_i$ and the kinetics of stomatal closure is not necessarily expected.

ABA Can Initiate Stomatal Closure through Ca^{2+}-Dependent and Ca^{2+}-Independent Pathways

Perhaps our most intriguing observation is that stomatal closure triggered by ABA is not always accompanied by changes in $[Ca^{2+}]_i$. We have measured $[Ca^{2+}]_i$ in 54 cells induced to close by ABA. In every case, closure was observed, but definite changes in $[Ca^{2+}]_i$ were observed in only 14 of them (all photometry measurements). Two possible explanations may account for the data differences between the photometry and the imaging results. First, the sampling interval (2.5 min) in the imaging data may have missed short transient changes in $[Ca^{2+}]_i$. Second, the two sets of data were obtained at different times of the year. The photometry measurements were gathered over a 6-month period from May to November 1989, whereas the imaging attempts covered August 1989 to January 1990. A seasonal variation in some aspects of stomatal function has been reported, particularly in plasma membrane ATPase activity (Blatt, 1990; Fricker and Willmer, 1990). The difference may be attributable to a different metabolic poise in the guard cell at these times.

This does not alter our finding that the great majority of cells do not alter their $[Ca^{2+}]_i$ levels but always close in response to ABA. This finding is clearly at variance both with what has been hypothesized for many years (Mansfield et al., 1990) concerning the transduction of ABA signals and with the conclusions from the data of McAinsh et al. (1990). Using photometric measurements on only 10 cells, they reported that eight cells responded to ABA with an increase in $[Ca^{2+}]_i$. The remaining two cells did not increase their $[Ca^{2+}]_i$ but closed in response to ABA (although the authors did not comment on this). Neither our data nor theirs would support an absolute requirement for ABA-induced elevation of $[Ca^{2+}]_i$ for closure.

Several explanations are possible. ABA could induce a change in the sensitivity of the guard cell to Ca^{2+} by way of phosphorylation or release of calmodulin, as suggested by Hepler and Wayne (1985). Alternatively, ABA may have metabolic effects that do not directly involve $[Ca^{2+}]_i$ but simply require a functioning Ca^{2+} system for the response. For example, Schauf and Wilson (1987) showed that ABA stimulated the opening of K^+ channels when applied to the cytoplasmic face of an excised membrane patch under constant (although high) Ca^{2+}. Blatt et al. (1990) also suggested that Ca^{2+} may promote the opening of K^+ efflux channels while inhibiting the activity of channels believed to mediate K^+ uptake. Another possibility is that ABA may act by way of either parallel or bifurcating pathways, one involving Ca^{2+}, that can initiate closure. The inositol system might fit into the latter category. Regardless, one cannot deduce a simple transduction scheme—ABA to Ca^{2+} to closure—from our data, and a more complex solution must be sought.

Our observations suggest that individual guard cells differ from one another in their biochemistry: some change their $[Ca^{2+}]$ but most do not. Although the patchiness of the guard cell response on an individual leaf is now accepted (Mansfield et al., 1990), we have observed an individual biochemical variation with the similar physiological response of closure. Fluorescence ratio analysis of single living plant cells can, therefore, be used with probes for Ca^{2+} (and possibly other ions as well) to examine this exciting biological variation at the molecular level.

METHODS

Fluorescent Dyes and Chemicals

Fluorescent dyes were obtained from Molecular Probes Inc. (Eugene, OR). Unless stated otherwise, all other chemicals were of analytical grade or higher and supplied either by Sigma (Poole, Dorset, United Kingdom) or British Drug House (Poole, Dorset, U.K.). Water (Hypersolv with free Ca^{2+} specified at about 100 nM) was purchased from British Drug House and used throughout.

Plant Material

Commelina communis plants were grown from seed in John Innes No. 2 potting compost under greenhouse conditions at 15°C to

25°C with a 16-hr day length. Experiments were performed between 10 AM and 4 PM to minimize the effects of diurnal rhythms in stomatal responses. The first or second fully expanded leaves on the main axis of 4-week-old to 5-week-old plants were excised and floated on distilled water for 30 min under continuous illumination (photon flux density, 100 μmol m^{-2} sec^{-1}, 400 m M to 700 mM) to open the stomata fully before experimentation. Abaxial (lower) epidermis (approximately 10 × 5 mm) was peeled off and floated on CO_2-free medium (50 mM KCl, 20 μM $CaCl_2$, 1 mM Mes, pH 6.1) under illumination for 30 min. CO_2-free air was obtained by passing air through a column of self-indicating soda lime.

Microscope Sample Chamber and Perfusion System

Each epidermal strip was mounted on a No. 1 coverslip (Chance Propper Ltd., Warley, U.K.) with a thin smear of silicone grease (high vacuum grease type 970 V, Dow Corning Corp., Midland, MI) around its periphery. This provided rigid attachment of the epidermis to the coverslip, which was essential to prevent specimen movement during microinjection. The center of the strip was grease free and used for measurements. The coverslip holding the epidermis formed the bottom of a circular, 20-mm diameter, open perfusion chamber (2-mL volume) continuously perfused with incubation medium at 5 mL/min. The medium was kept CO_2 free by bubbling the reservoir of the perfusion system with CO_2-free air, which was also passed as a stream over the perfusion chamber surface. Temperature was monitored with a thermocouple (Y8104 thermocouple, John Fluke Inc., Tilburg, The Netherlands) in the chamber and regulated at 25°C by immersing the perfusion reservoir in a temperature-controlled water bath. To minimize any dark-induced closure of guard cells, the sample chamber was illuminated continuously at a wavelength of 600 nm using the microscope's transmitted light source (12-V tungsten lamp) and a 600-nm, 10-nm half-bandwidth, interference filter (Ealing Electro-optics, Watford, U.K.). Light at this wavelength did not interfere with the quantitative measurements made at wavelengths below 500 nm for fluorescence ratio analysis of Indo-1.

Microinjection of Indo-1 into Guard Cells

Micropipettes were pulled from filament electrode glass (Clark electromedical GC105F, Clark Electromedical Instruments, Reading, Great Britain). Micropipette tip diameters were 0.31 ± 0.06 μM (n = 20). For microinjection the micropipette was filled with 100 μM Indo-1. Cells were injected by ionotophoresis at less than 0.1 nA for 5 min to 10 min. The most successful cytosolic injections were performed on guard cells of stomata between 10 μM and 15 μM aperture size. Microinjection of guard cells surrounding closed stomata generally led to injection into the vacuole. Removal of the injecting pipette from fully open (20 μM stomatal aperture) guard cells was accompanied by a small but obvious loss of turgor. Injected cells were left for 15 min to ensure complete diffusion of the dye throughout the cytoplasm.

Estimation of Intracellular Indo-1 Concentration

The cytosolic concentration of Indo-1 injected into the guard cells was estimated by comparison of the fluorescence intensity at the isobestic ([Ca^{2+}]-independent) wavelength with the signal from a range of concentrations of Indo-1 in small droplets of calibration solution. The droplets were formed by pressure injection into a 1-mm layer of silicone oil to give a similar volume to a guard cell (approximately 6 pL).

Fluorescence Ratio Analysis

Microscope System

The ratio analysis system is based on a modified Nikon-Diaphot inverted epifluorescence microscope fitted with 340-nm transmissive optics and a 75-W xenon epifluorescence lamp. A quartz ND 3 (1/8 transmittance) neutral density filter (Ealing Electro-optics) was used to reduce the intensity of the excitation light. The excitation wavelength was determined by a 350-nm, 10-nm half-bandwidth, interference filter (Ealing Electro-optics) mounted in a motor-driven excitation filter wheel (Newcastle Photonic Systems, Newcastle-upon-Tyne, U.K.) installed on the front of the Nikon epicondenser. A Nikon CF Fluor DL 40×, 0.85 numerical aperture, 0.37-mm working distance, dry objective was used routinely. Oil immersion lenses proved unsatisfactory with our guard cell material because (1) direct contact with the coverslip often caused slight movements of the specimen that prevented the precise registration of sequences of images essential for ratio imaging, and (2) working distances were often too limited. A Nikon 400-nm dichroic mirror allowed fluorescent light from the specimen to pass to the microscope side port. Emission filtrations for the photometric and imaging system were different (see below). Imaging and photometry measurement were from the midplane of the cell.

Photometric System

A standard Nikon variable aperture and PFX shutter system were placed on the emission side port of the microscope. A Nikon 430-nm dichroic mirror was positioned after the shutter assembly and light of wavelengths below 430 nm and above 430 nm passed through a 405-nm or 480-nm, 10-nm half-bandwidth, interference filter (Ealing Electro-optics), respectively. Two 9924a photomultipliers (Thorn-EMI, Middlesex, U.K.), selected for extremely low dark current (less than 0.1 nA), were used to detect the light at each of these wavelengths. The photomultiplier signals were passed to a dual photon counter (Newcastle Photonic Systems) and analyzed online with a BBC Master computer (Acorn Computers Ltd., Cambridge, U.K.) using software modified from that supplied by Newcastle Photonic Systems. The system was configured to acquire data continuously and to calculate a ratio of the photomultiplier signals every second. An online autofluorescence subtraction was performed at each wavelength before ratio calculation using the autofluorescence signal measured from the guard cell under study before it was microinjected. Typically, the measurement aperture covered the whole guard cell pair to allow for changes in guard cell shape and position during stomatal responses.

Imaging System

A motor-driven filter wheel (Newcastle Photonic Systems) replaced the photomultiplier system described above on the side port of the microscope. This allowed computer-controlled switching between any of three interference filters and a blank in the

emission light path. Images were recorded using an Extended-ISIS intensified CCD camera (Photonic Science, Kent, U.K.) and digitized using a Synapse frame store controlled by the Semper-6-Plus image processing language (Synoptics Ltd., Cambridge, U.K.) running on a Dell 310 microcomputer equipped with a maths coprocesser (Dell Corp., Berkshire, U.K.). The frame store applied a 0.5-sec recursive filter to the incoming image to increase the signal-to-noise ratio. Images were stored on a 90-megabyte hard disc before analysis. The camera's intensifier and video gains were set to 50% of maximum, which provided the best compromise between signal amplification and image noise. All images were recorded from the central 50% of the camera's field of view, which showed no detectable blemishes or inhomogeneities in sensitivity or illumination. For Indo-1 measurements, the filter wheel was switched between a 415-nm and 480-nm interference filter (both 10-nm half-bandwidth, Ealing Electro-optics) for collection of data for ratio calculations and an ND 3 neutral density filter for acquisition of the corresponding bright-field image. Switching between filters and subsequent image capture took approximately 1 sec. The excitation filter wheel was moved to the blank position between each active image capture cycle to cut off the 350-nm excitation beam. This procedure reduced the photobleaching of the Indo-1 throughout the experiment and minimized cell exposure to excitation light. Data for ratio images were recorded every 2.5 min. Using the 40× lens, each image pixel represented 0.4 μm.

Image Processing

Image processing and ratio calculation were performed using the Semper-6-Plus image processing language. The fluorescence image at each wavelength comprised three components: (1) a constant camera dark current, (2) an autofluorescence signal from the cell, and (3) the signal from the intracellular Indo-1. Image processing was performed to minimize the contribution of the first two factors to the final image used for ratio calculations. The signal from the camera dark current was subtracted from all images. The images at each wavelength were then corrected for autofluorescence before ratio calculation. A simple subtraction of the image of the autofluorescence from the cell before dye microinjection is generally not feasible because the precise registration of images before and after dye loading, which is essential for such a subtraction to work, cannot be guaranteed. Similarly, autofluorescence is not uniform throughout the cell and changes with stomatal and organellar movements. Thus, an alternative, more applicable autofluorescence correction was developed. Autofluorescence was averaged over a 9 × 9 array of pixels detected from the cytoplasm just beside the nucleus in the noninjected guard cell of the guard cell pair. This value was then subtracted from the whole image. The noninjected guard cell represents the closest analog of the injected cell, being part of the same stomatal apparatus and, therefore, most likely to represent the autofluorescence signal found in the loaded cell. Similar calculations of autofluorescence comparing two noninjected guard cells around a stoma showed deviations of 6 ± 4% (n = 15) between the two. Each image of a guard cell pair contains a loaded and unloaded guard cell, so autofluorescence was calculated independently for each image throughout the time course of the experiment. Thus, changes in autofluorescence during the course of the experiment from photobleaching, for example, were automatically taken into account. This autofluorescence calculation corrects cytosolic regions for autofluorescence but may not be correct for other cellular regions. The chloroplast and vacuolar autofluorescences were not evident at the wavelengths used for fluorescence ratio analysis of Indo-1 (Figure 2). However, autofluorescence from the t-shaped junction of the guard cells and the wall forming the inner lip of the stomatal pore represented from 10% to 30% of the fluorescence signal from cytosolic Indo-1 in loaded cells (Figure 2). This would be sufficient to underestimate the true $[Ca^{2+}]_i$ in cytoplasm in these regions by 10% to 20%. The autofluorescence correction detailed is the most applicable cytosolic correction we have been able to devise. Ratio images calculated from data not corrected for autofluorescence underestimated Ca^{2+} levels by typically 25% in the cytosolic regions.

After autofluorescence correction, a mask was defined for each image that excluded regions where the final signal strength was below that known to give reliable ratio results, such as the thin cytoplasm over the vacuole. This level was determined by performing calibrations (see below) with the signal strength progressively reduced with neutral density filters until the ratio differed by >10% from those obtained with high signal strength. The grey level value of each pixel in the masked image at 405 nm was divided by the value of each corresponding pixel in the masked image at 480 nm. The resulting ratio image was color coded to represent different Ca^{2+} concentrations determined after calibration (see below). Floating point arithmetic was used throughout

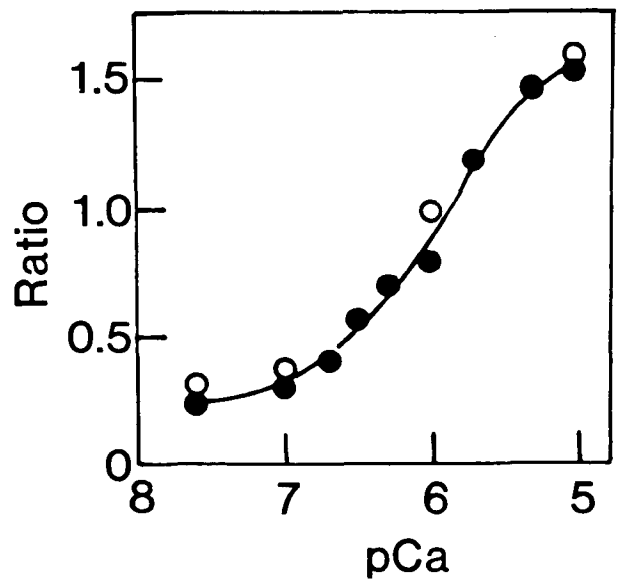

Figure 8. In Vitro (●) and in Vivo (○) Calibration of Photometric Indo-1 Ratio Measurements Versus Free Ca^{2+} Concentration.

For the in vitro calibration, the buffer, containing 0.5 μM Indo-1, 100 mM KCl, 1 mM $MgCl_2$, 10 mM Hepes (pH 7.0), 10 mM EGTA, and the appropriate amount of $CaCl_2$ to give the required free Ca^{2+} concentration, was perfused through the sample chamber, and the ratios were calculated. For the in vivo calibration, Indo-1-loaded guard cells were treated with 10 μM Br-A23187 and 10 mM EGTA with appropriate amounts of $CaCl_2$ to give the required free Ca^{2+}.

the ratio calculation. Hard copies of the images were produced using a Mitsubishi CP 100B video copy processor.

Calibration of Ratio Versus Ca^{2+} Concentration

An in vitro (external) calibration of ratio versus free Ca^{2+} concentration was performed using Ca^{2+}-EGTA buffers to set the free Ca^{2+} level. Calibration buffers contained 0.5 μM Indo-1, 100 mM KCl, 1 mM $MgCl_2$, 10 mM Hepes (pH 7.0), 10 mM EGTA, and appropriate $CaCl_2$ to give the required free Ca^{2+} concentration (Gilroy et al., 1989). These solutions were perfused through the sample chamber and the ratio was calculated with either the photometry or imaging equipment. Standard curves were constructed independently for each of these systems. In vivo (internal) calibrations were performed on dye-loaded guard cells treated with 10 μM Ca^{2+} ionophore Br-A23187, which exhibited negligible fluorescence at the wavelengths analyzed. It was assumed that internal free Ca^{2+} reached equilibrium with the external Ca^{2+} level after 10 min of ionophore treatment. Similar results were obtained with ionomycin but required a 10-fold higher concentration of the ionophore. Close agreement between internal and external calibrations is not always seen (Gilroy et al., 1990). However, in this case, the in vivo calibrations agreed with those performed in vitro by >90% and are shown in Figure 8. Thus, the continuous perfusion with calibration solution maintained during the in vivo calibration of the guard cells apparently efficiently equilibrated internal and external Ca^{2+} levels. Therefore, the in vitro calibrations were routinely used to calculate Ca^{2+} concentrations in view of their simplicity and reliability (Gilroy et al., 1989).

ACKNOWLEDGMENTS

This research was supported by grants from the Science and Engineering Research Council, the Agricultural and Food Research Council, and the Gatsby Foundation.

Received November 14, 1990; accepted February 5, 1991.

REFERENCES

Alexandre, J., Lassales, J.P., and Kado, R.T. (1990). Opening of Ca^{2+}-channels in isolated red beet vacuole membrane by inositol-1,4,5-triphosphate. Nature **343,** 567–570.

Atkinson, C.J., Mansfield, T.A., Kean, A.M., and Davies, W.J. (1989). Control of stomatal aperture by calcium in isolated epidermal tissue and whole leaves of *Commelina communis*. New Phytol. **111,** 9–17.

Berridge, M.J., and Irvine, R.F. (1989). Inositol phosphates and cell signalling. Nature **341,** 197–205.

Blatt, M.R. (1985). Extracellular potassium activity in attached leaves and its relation to stomatal function. J. Exp. Bot. **36,** 240–251.

Blatt, M.R. (1990). Potassium channel currents in intact stomatal guard cells: Rapid enhancement by abscisic acid. Planta **180,** 445–455.

Blatt, M.R., Thiel, G., and Trentham, D.R. (1990). Reversible inactivation of K^+ channels of *Vicia* stomatal guard cells following the photolysis of caged inositol-1,4,5-triphosphate. Nature **346,** 766–769.

Bowling, D.J.F. (1987). Measurement of the apoplastic activity of K^+ and Cl^- in the leaf epidermis of *Commelina communis* in relation to stomatal activity. J. Exp. Bot. **38,** 1351–1355.

Bush, D.S., and Jones, R.L. (1988). Measurement of cytoplasmic calcium in aleurone protoplasts using Indo-1 and Fura-2. Cell Calcium **8,** 455–472.

Bush, D.S., and Jones, R.L. (1990). Measuring intracellular Ca^{2+} levels in plant cells using the fluorescent probes Indo-1 and Fura-2. Plant Physiol. **93,** 841–845.

Cobbold, P.H., and Rink, T.J. (1987). Fluorescence and bioluminescence measurement of cytoplasmic free calcium. Biochem. J. **248,** 313–328.

Davies, W.J., Wilson, J.A., Sharp, R.E., and Osonubi, O. (1981). Control of stomatal behaviour in water stressed plants. In Stomatal Physiology, P.G. Jarvis and T.A. Mansfield, eds (Cambridge, UK: Cambridge University Press), pp. 163–185.

De Silva, D.L.R., Cox, R.C., Hetherington, A.M., and Mansfield, T.A. (1985a). Suggested involvement of calcium and calmodulin in the responses of stomata to abscisic acid. New Phytol. **101,** 555–563.

De Silva, D.L.R., Hetherington, A.M., and Mansfield, T.A. (1985b). Synergism between calcium ions and abscisic acid in preventing stomatal opening. New Phytol. **100,** 473–482.

Elliott, D.C., and Petkoff, H.S. (1990). Measurement of cytoplasmic free calcium in plant protoplasts. Plant Sci. **67,** 125–131.

Fricker, M.D., and Willmer, C.M. (1990). Some properties of protein pumping ATPases at the plasma membrane and tonoplast of guard cells. Biochem. Physiol. Pflanzen., in press.

Fricker, M.D., Gilroy, S., Read, N.D., and Trewavas, A.J. (1991). Visualisation and measurement of the calcium message in guard cells. In Molecular Biology of Plant Development, W. Schuch and G. Jenkins, eds (Cambridge, UK: The Company of Biologists Ltd.), in press.

Gilroy, S., Hughes, W.A., and Trewavas, A.J. (1989). A comparison between Quin-2 and aequorin as indicators of cytoplasmic calcium levels in higher plant cell protoplasts. Plant Physiol. **90,** 482–491.

Gilroy, S., Read, N.D., and Trewavas, A.J. (1990). Elevation of cytoplasmic calcium by caged calcium or caged inositol triphosphate initiates stomatal closure. Nature **346,** 769–771.

Grynkiewicz, G., Poenie, M., and Tsien, R.Y. (1985). A new generation of calcium indicators with greatly improved fluorescence properties. J. Biol. Chem. **260,** 3440–3450.

Hedrich, R., and Neher, E. (1987). Cytoplasmic calcium regulates voltage-dependent ion channels in plant vacuoles. Nature **329,** 833–835.

Hedrich, R., and Schroeder, J.I. (1989). The physiology of ion channels and electrogenic pumps in higher plants. Annu. Rev. Plant Physiol. **40,** 539–569.

Hedrich, R., Barbier-Brygoo, H., Felle, H., Flugge, U.I., Luttge, U., Maathius, F.J.M., and Zeiger, P. (1988). General mecha-

nisms for solute transport across the tonoplast of vacuoles: A patch clamp survey of ion channels and proton pumps. Bot. Acta **101,** 7–13.

Hepler, P.K., and Wayne, R.O. (1985). Calcium and plant development. Annu. Rev. Plant Physiol. **36,** 397–439.

Inoue, H., and Katoh, Y. (1987). Calcium inhibits ion stimulated opening in epidermal strips of *Commelina communis* L. J. Exp. Bot. **38,** 142–149.

Irvine, R.F. (1990). Second messenger gets the green light. Nature **346,** 700–701.

Keller, B.U., Hedrich, R., and Raschke, K. (1989). Voltage dependent anion channels in the plasma membrane of guard cells. Nature **341,** 450–453.

MacRobbie, E.A.C. (1988). Control of ion fluxes in stomatal guard cells. Bot. Acta **101,** 140–149.

MacRobbie, E.A.C. (1989). Calcium influx at the plasmalemma of isolated guard cells of *Commelina communis*. Planta **178,** 231–241.

Mansfield, T.A., Hetherington, A.M., and Atkinson, C.J. (1990). Some current aspects of stomatal physiology. Annu. Rev. Plant Physiol. **41,** 55–75.

McAinsh, M.R., Brownlee, C., and Hetherington, A.M. (1990). Abscisic acid-induced elevation of guard cell Ca^{2+} precedes stomatal closure. Nature **343,** 186–188.

Nejidat, A. (1987). Effect of ophiobolin A on stomatal movement: Role of calmodulin. Plant Cell Physiol. **28,** 455–460.

Nejidat, A., Roth-Bejerano, N., and Itai, C. (1986). Mg-ATPase activity in guard cells of *Commelina communis*. Physiol. Plant. **68,** 315–319.

Raschke, K. (1975). Stomatal action. Annu. Rev. Plant . Physiol. **26,** 309–340.

Schauf, C.L., and Wilson, K.J. (1987). Effects of abscisic acid on K^+ channels in *Vicia faba* guard cell protoplasts. Biochem. Biophys. Res. Commun. **145,** 284–290.

Schroeder, J.I., and Hagiwara, S. (1989). Cytosolic calcium regulates ion channels in the plasma membrane of *Vicia faba* guard cells. Nature **338,** 427–430.

Schroeder, J.I., and Hedrich, R. (1989). Involvement of ion channels and active transport in osmoregulation and signalling of higher plant cells. Trends Biochem. Sci. **14,** 187–192.

Schwartz, A. (1985). Role of Ca^{2+} and EGTA on stomatal movements in *Commelina communis* L. Plant Physiol. **79,** 1003–1005.

Schwartz, A., Ilan, N., and Grantz, D.A. (1988). Calcium effects on stomatal movement in *Commelina communis* L. Plant Physiol. **87,** 583–587.

Smith, G.N., and Willmer, C.M. (1988). Effect of calcium and abscisic acid on volume changes of guard cell protoplasts of *Commelina*. J. Exp. Bot. **39,** 1529–1539.

Speksnijder, J.E., Miller, A.L., Weisenseel, M.H., Chen, T.-H., and Jaffe, L.F. (1989). Calcium buffer injections block fucoid egg development by facilitating calcium diffusion. Proc. Natl. Acad. Sci. USA **86,** 6607–6611.

Thomas, M.V. (1982). Techniques in Calcium Research. (London: Academic Press).

Tsien, R.Y., and Poenie, M. (1986). Fluorescence ratio imaging: A new window into intracellular ionic signalling. Trends Biochem. Sci. **11,** 450–455.

Weyers, J.D.B., Paterson, N.W., Fitzsimons, P.J., and Dudley, J.M. (1982). Metabolic inhibitors block ABA induced stomatal closure. J. Exp. Bot. **33,** 1270–1278.

Zeiger, E. (1983). The biology of stomatal guard cells. Annu. Rev. Plant Physiol. **34,** 441–475.

Zhao, X.J., Sucoff, E., and Stadelmann, E.J. (1987). Al^{3+} and Ca^{2+} alteration of membrane permeability of *Quercus rubra* root cortex cells. Plant Physiol. **83,** 159–162.